

DiffusionRL: Efficient Training of Diffusion Policies for Robotic Grasping Using RL-Adapted Large-Scale Datasets

Maria Makarova¹
maria.makarova2@skoltech.ru

Qian Liu²
qianliu@dlut.edu.cn

Dzmitry Tsetserukou¹
d.tsetserukou@skoltech.ru^{*}

Abstract: Diffusion models have been successfully applied in areas such as image, video, and audio generation. Recent works show their promise for sequential decision-making and dexterous manipulation, leveraging their ability to model complex action distributions. However, challenges persist due to the data limitations and scenario-specific adaptation needs. In this paper, we address these challenges by proposing an optimized approach to training diffusion policies using large, pre-built datasets that are enhanced using Reinforcement Learning (RL). Our end-to-end pipeline leverages RL-based enhancement of the DexGraspNet dataset, lightweight diffusion policy training on a dexterous manipulation task for a five-fingered robotic hand, and a pose sampling algorithm for validation. The pipeline achieved a high success rate of 80% for three DexGraspNet objects. By eliminating manual data collection, our approach lowers barriers to adopting diffusion models in robotics, enhancing generalization and robustness for real-world applications.

Keywords: Diffusion Policy, Reinforcement Learning, Dexterous Manipulation

1 Introduction

Diffusion models have proven to be a powerful tool in the field of generative artificial intelligence successfully applied in image synthesis, video generation and audio generation [1, 2, 3, 4, 5]. Using an iterative denoising approach, these models learn to invert a diffusion process, transforming random noise into sophisticated, high-quality samples.

Reinforcement Learning (RL) and Imitation Learning (IL) have become particularly popular in the field of robot learning for the tasks of perceiving the environment and making decisions to perform actions in recent years [6]. But RL approach is highly dependent on the correct tuning of hyperparameters [7], and effective IL training requires a large amount of diverse high-quality data [8]. Also, the multimodal nature of complex robot tasks hinders the construction of stable control. More recently, researchers have begun to integrate an approach in the form of diffusion policy learning into the field of robotics as well.

The concept of diffusion policy was first introduced by Chi et al. [9]. The diffusion process has been applied to robot action sequence generation since such models are able to capture the complex multimodal distributions that are characteristic of many robotics tasks, as mentioned above. Diffusion

^{*}¹The authors are with the Intelligent Space Robotics Laboratory, Center for Digital Engineering, Skolkovo Institute of Science and Technology (Skoltech), 121205 Moscow, Russia.

[†]² Qian Liu is with the Department of Computer Science and Technology, Dalian University of Technology, Dalian, China.

models have found applications in constrained motion planning [10, 11], human-robot interaction (HRI) [12], mobile manipulation [13, 14] and navigation [15, 16].

They have also begun to be applied in dexterous robotic manipulation, which is one of the most demanded tasks. DexDiffuser [17] introduces DexSampler, which generates grasping poses based on the point cloud of a 3D object using the diffusion process. GraspGF [17] is an algorithm that uses a generative model as a primitive hand-object-conditional policy. DexGrasp-Diffusion [18] combines multi-dexterous hand grasp estimation with open-vocabulary setting to filter physically plausible functional grasps based on object affordances.

In other works [19, 20] authors utilize video demonstrations and Vision-Language-Action (VLA) models. In the latter work, the VLA provides high-level planning through language commands, while the diffusion model handles low-level interactions that ensure accuracy and robustness. The VLA guides the robot to the target object, after which the diffusion model implements ADAPT Hand 2 [21] grasping actions. The authors demonstrated that the model-switching approach yields more than 80% success rate compared to less than 40% using the VLA model alone. However, the diffusion model training dataset consisted of 30-40 samples for each scenario, which does not allow efficient generalization to other objects.

Therefore, we have decided to simplify the integration of this approach and provide the ability to train diffusion models based on large ready-to-use datasets containing various examples of object poses and actions for grasping. As such a dataset, we adopted the DexGraspNet [22] dataset for ShadowHand [23] with 24 degrees of freedom, containing 1.32 million capture examples for 5355 objects, covering more than 133 object categories and containing more than 200 different captures for each object instance. But this dataset cannot always be successfully applied to training on individual tasks. For example, the authors of DexDiffuser [17] also described a large percentage of inaccurate samples, reaching more than 50%.

We developed an end-to-end pipeline that allows to efficiently train lightweight diffusion policies on existing datasets customized for specific tasks and environmental conditions using an RL agent, significantly reducing the need for manual data collection in complex manipulation tasks and increasing scalability. The main contributions of the presented work can be summarized as follows:

- A pipeline was developed to enhance the DexGraspNet samples using a lightweight RL model in a changing robot pose scenario. The resulting high quality dataset was used to train a diffusion model in the dexterous grasping task with the ShadowHand robotic hand.
- To validate the success of the training, an algorithm was developed to generate random object poses based on the statistics of the original DexGraspNet dataset.
- A compact diffusion model was trained on three different objects, and its performance in grasping objects in random scenarios reached a high value of about 80%.

Our method can be used in a large set of real-world complex robotic manipulation tasks, as it allows to train lightweight diffusion models on large-scale pre-built datasets, adapting them to specific conditions without the need to collect extensive data manually.

2 Methods

2.1 Dataset Enhancement with Reinforcement Learning

The training of a diffusion model for grasping complex objects located in the workspace of the UR10e robot is based on the DexGraspNet dataset. Simply transferring this dataset to the simulation environment to train the diffusion model is a problematic. For example, the application of some object and hand poses depends on a specific hand position, as shown in Fig. 1. If the hand pose is changed, the stability of the object during grasping will be compromised. In addition, the gripper models in the dataset and the simulated environment have small discrepancies, resulting in instability.

Therefore, to effectively train the diffusion model, an RL agent was built to **predict additional grasping actions** in addition to those taken from the original dataset. These actions are designed to provide reliable and stable object grasping in different poses of the UR10e robot.

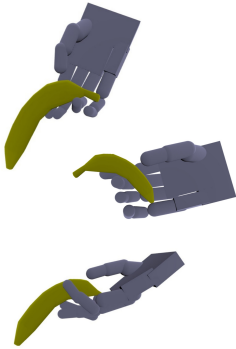


Figure 1: Inappropriate DexGraspNet samples.

The process of enhancing the dataset is depicted schematically in Fig. 2(a). First, samples of the dataset were manually selected based on visual criteria to exclude the poses shown in Fig. 1. Next, the RL agent was then trained to predict additional actions in the static pose of the UR10e robot when the palm of the gripper is in a vertical orientation. This approach was used to determine which samples from the dataset could not be improved by the RL agent even in static pose. The samples from the dataset selected in these two steps were used to train the RL agent to predict additional actions in the conditions of the UR10e robot’s pose variation at the beginning of each episode.

Reinforcement Learning Agent

After positioning the UR10e robot arm at the beginning of each episode, the position of the object was recalculated based on a sample from the dataset by calculating inverse positional and rotational transformations from the gripper. The object was placed in the calculated region in front of the gripper in the absence of gravity. After the object is placed, the motion of the gripper joints from the DexGraspNet dataset is realized, followed by an additional motion of the gripper joints predicted by the RL agent. Gravity is then enabled and the grasp validation is performed: if the object has not fallen out of the gripper, the validation is successful, and vice versa. The scheme of the described process is shown in Fig. 2(b). Training was based on the Twin Delayed DDPG (TD3) algorithm [24]. The Critic and Actor models were built as lightweight architectures consisting of four linear layers each (Fig. 3).

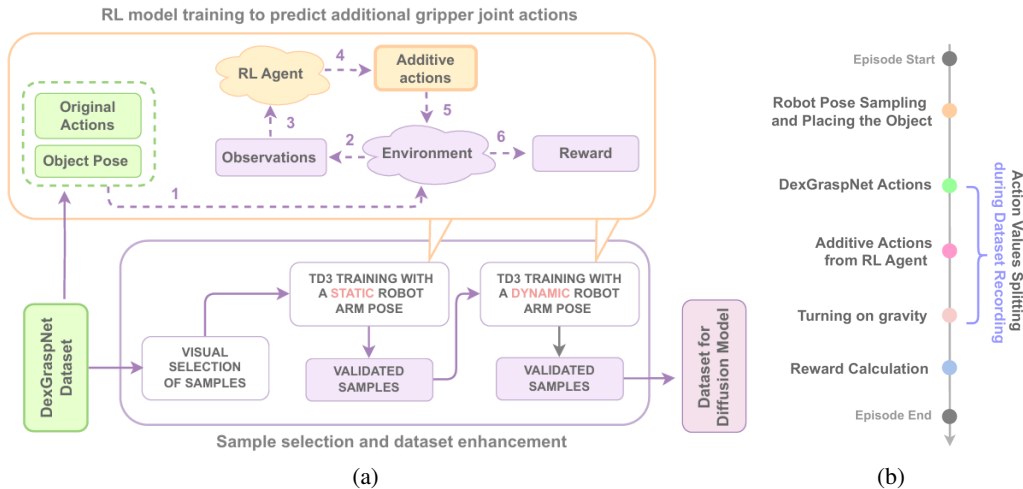


Figure 2: (a) RL-based Dataset Enhancement Pipeline. The numbers indicate the data flow sequence during the training of the RL agent: from DexGraspNet, the data on the object pose and actions for the gripper are sent to the Environment (1), from where the Observations vector is received by the RL agent (2, 3), after which it predicts additional gripper actions for the Environment (4, 5), where the final Reward is calculated to validate the success of the object grasping process (6); (b) Environmental Timestamps Details during RL-agent Training and Dataset Recording.

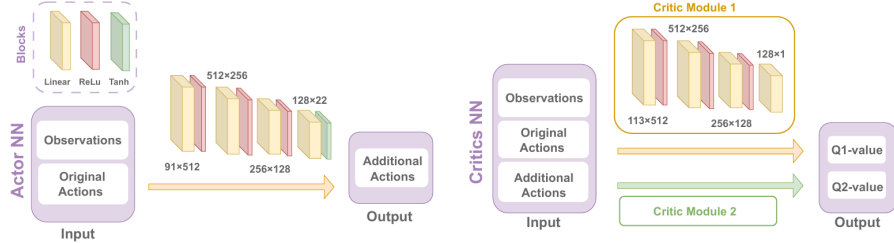


Figure 3: Actor and Critics Neural Networks architectures.

2.2 Diffusion Model

The environment differs from the previously described one in that information from DexGraspNet samples in the form of object position and gripper joint actions are no longer used. The placement of the object in front of the gripper is accomplished using a pose sampling algorithm, which will be described below. The sequence of actions is predicted directly by the diffusion model.

As in the original work on Diffusion policy [9], the samples of the dataset have been transformed. The DDPM model [25] uses the observation history of the 2 previous steps, predicts 8 action vectors, and implements half of them in the environment. For vectors that precede the initial vectors in the episode, the context is duplicated by the initial vectors. Similarly, for the final vectors, the context is duplicated by them. An illustration for a recalculated sample is shown in Fig. 5. The model architecture was constructed as a Conditional U-net (Fig. 4), as proposed in the original paper [26, 9].

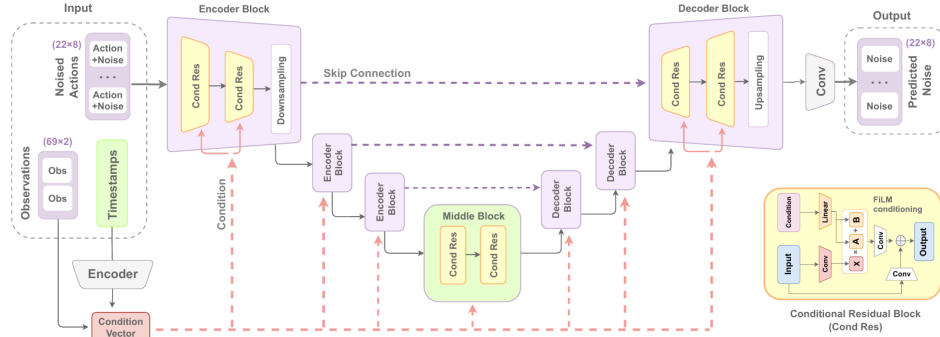


Figure 4: Diffusion Model Conditional U-net Architecture. Conditional Residual Blocks are highlighted in yellow.

3 Experiments

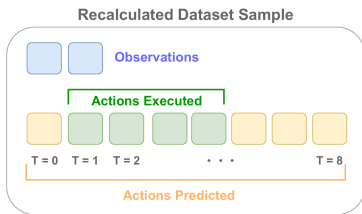


Figure 5: Recalculated Dataset Sample.

Environment description

The environment built in ManiSkill [27] contains a UR10e robot and a ShadowHand robotic hand located on it. The UR10e robot has 6 joints, the ShadowHand has 24 joints. At the beginning of each episode, the robot's position is set for all 6 joints of the UR10e ($i = 1, \dots, 6$) and for the 2 joints of the gripper connecting the palm to the wrist and the wrist to the forearm ($i = 7, 8$). The values of the joint angles vary by A_i from the initial value of joint S_i , characterizing its values for the static position of the robot (the gripper's palm is in a vertical position). These values for each

of the 8 joints are: $[A_1, \dots, A_8] = [\pi/2; \pi/12; \pi/12; \pi/12; \pi/8; \pi/8; \pi/8; \pi/8]$; $[S_1, \dots, S_8] = [0; -\pi/2; 3\pi/4; -3\pi/4; \pi/2; -\pi; 0; 0]$. The formula for calculating the resulting values of joint angles is $R_i = S_i + w_i * A_i$, where w_i is a random number from $[-1; 1]$.

The *Action* vector for the RL agent is of size 22 and is used to control the gripper joints except for the two previously described. The *Observation* vector for the agent consists of all 30 values of the angles of the robot and gripper joints, the object position (translation vector and rotation quaternion) relative to the gripper base, the initial global position of the object at the beginning of the episode, the current global position of the object, the global position of the gripper base, and the global translation vectors of the five joints of the upper phalanges of the gripper. In addition to these values, the RL agent receives 22 values characterizing the values of the grip joint angles from DexGraspNet. Thus, the final Observations vector has a size of 91. The *Reward* was chosen to be sparse and calculated as follows: $Reward = -1$ if the vertical coordinate of the object deviated from the coordinate set at the beginning of the episode by an amount greater than $d = 0.025$ after gravity was turned on, and $Reward = 0$ otherwise. All objects of the same type (Banana, Bottle and Camera) are considered at a single scale, which was calculated as the average value for that object in the original dataset.

3.1 RL Agent Training.

As described in Section 2.1, after visual selection of samples from DexGraspNet, the RL agent was trained to predict additional actions for the gripper joints when the robot is static (with the gripper’s palm upright). The training results are summarized in Fig. 6(a) and Fig. 6(b). As can be seen, the agent was not completely successful because not all samples from the dataset could be effectively improved with RL. Some samples were too imprecise and additional actions did not help in object grasping. Therefore, they were also excluded from the dataset. The remaining samples were used to train the RL agent with the robot pose dynamically changing at the beginning of each episode. The training results are shown in Fig. 6(c) and Fig. 6(d).

The results demonstrate that the RL agent was successfully trained and achieved convergence close to 90-100% success rate. Training of the RL-agent in each of the experiments occurred over 200 epochs of 75 episodes each.

A dataset of 2000 episodes was then recorded for each object. The actions for the gripper joints were limited to 25×10^{-4} for each time step for smoother motion, which is important for the robustness of the diffusion model training (Fig. 2(b)). The statistics of the number of successful trajectories when collecting the new dataset for each object are summarized in the Table 1, as are the statistics of the number of samples collected after visual selection and training with a stationary robot arm. The dataset now contains high-quality samples and is suitable for training the diffusion model.

Object	DexGraspNet Samples	Ratio after Visual Selection	Ratio after Training on a Static Robot	New Dataset Successful Samples Rate
Banana	205	54%	42%	93%
Bottle	248	66%	42%	96%
Camera	206	49%	32%	96%

Table 1: Statistics for Dataset Samples Collected during the Dataset Enhancement and Recording Process.

3.2 Algorithm for Sampling Object Poses

To evaluate the efficiency of training the diffusion model, it was necessary to implement an algorithm for generating poses of objects that were not included in the training dataset. It is important that these poses are realistic and diverse. Considering that the DexGraspNet dataset was used in this work, since it contains such examples, it was decided to build an algorithm for sampling poses based on the statistics of the available data from it. First, for each of the three objects, statistics were collected on the values of three coordinates and three Euler angles of rotation relative to the gripper. Only

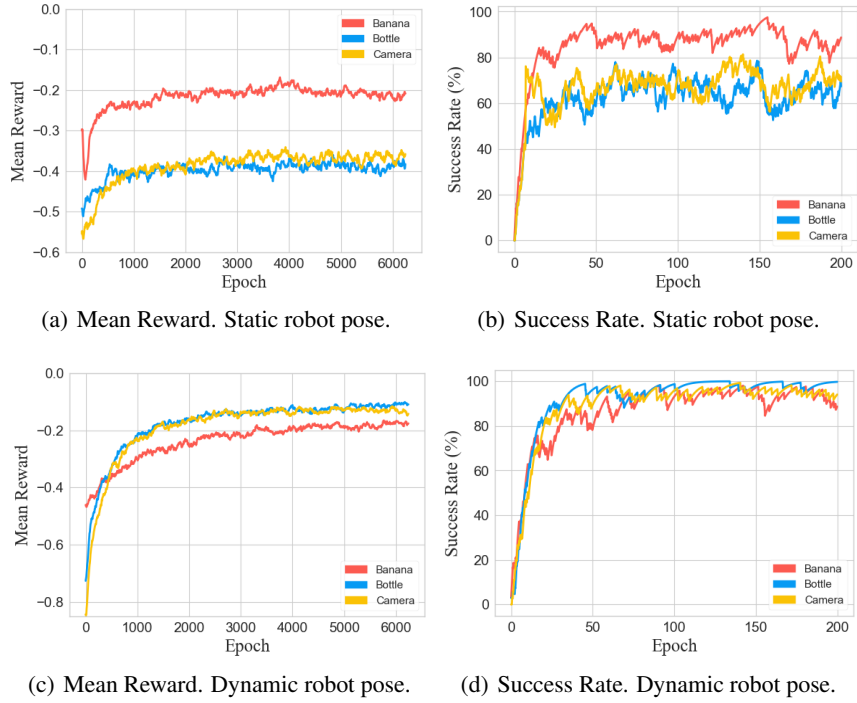


Figure 6: Mean Reward and Mean Success Rate values during training an RL agent with static and dynamic robot pose to predict additional gripper actions. Success Rate means mean percentage of transitions that have a success reward during validation. Training with dynamic robot pose was performed on a subset of the data selected after training with static robot pose.

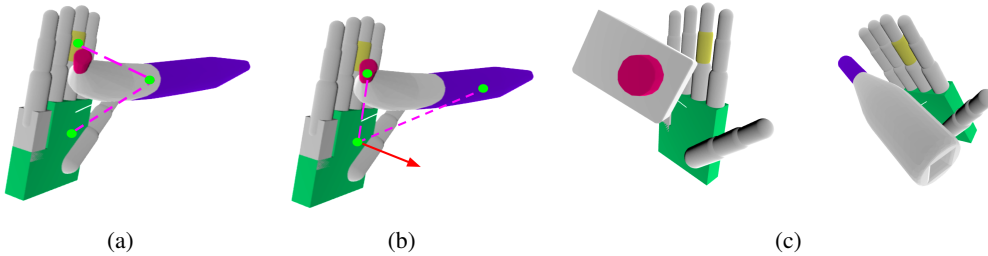


Figure 7: (a) Metrics of distances from the middle phalanx of the middle finger and the palm of the gripper's hand to the center of the object; (b) Metric of the angle between the directions to the edges of an oblong object and the vector of normal to the palm of the hand; (c) Examples of pose sampling for Bottle and Camera objects.

those samples from the dataset that were used to train the RL agent with a dynamically changing robot pose were taken into account. The statistics are shown in Fig. 8(a), Fig. 8(b).

Since random selection of coordinate and rotation values from the calculated distribution was unsuitable for pose generation, we introduced metrics for pose validation. To estimate the distance to a realistic grip area, we measured two values: the distance from the middle phalanx of the middle finger and from the center of the palm to the object (Fig. 7(a), Fig. 8(c)). We also computed the minimum distances between all points of these considered gripper parts and the object (Fig. 8(d)). For oblong Banana object, we added angular boundary metrics between the vectors pointing to its edges and the palm's normal vector (Fig. 7(b), Fig. 8(e)).

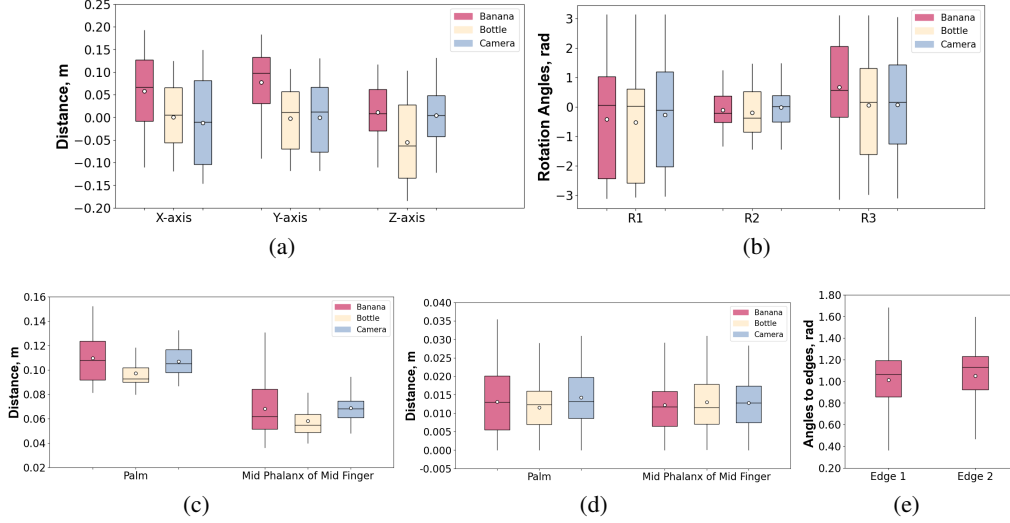


Figure 8: (a) – Distribution of axial distances between the gripper and the object; (b) – Distribution of angles of rotation of the gripper relative to the object; (c) – Distances between the centers of the considered parts of the gripper and the object; (d) – Minimum distances between any point of the considered parts of the gripper and the object; (e) – Angles between the normal vector of the palm and the directions to the edges of the Banana object.

The values of coordinates and rotation angles for each object were sampled from a uniform distribution $\mathcal{U}(a, b)$, where a and b are defined as follows:

$$a = \frac{Q_1 + L}{2}, \quad b = \frac{Q_3 + U}{2},$$

with L and U being the boxplot whiskers: $L = Q_1 - 1.5 \times \text{IQR}$, $U = Q_3 + 1.5 \times \text{IQR}$, Q_1 and Q_3 are the first and third quartiles (boxplot bounds), $\text{IQR} = Q_3 - Q_1$ is the interquartile range.

The boundary values for the distances between the centers of the palm and middle phalanx of the middle finger to the object were calculated as $D_{max} = Q_3 + 1.5 \times \text{IQR}$. The minimum allowable distances between any points of these parts of the gripper and the object were calculated as $D_{min} = Q_1 - 1.5 \times \text{IQR}$. For the Banana object, it was checked that the angles of directions to its edge parts lie in the range from $\theta_{min} = Q_1 - 1.5 \times \text{IQR}$ to $\theta_{max} = Q_3 + 1.5 \times \text{IQR}$.

Finally, the sampled object poses were additionally checked for collisions with the gripper.

3.3 Diffusion Model Training.

After collecting the dataset and processing it as described in Section 2.2, the diffusion model was trained on three objects: Banana, Bottle and Camera. The number of training iterations for each of the objects was 100 000, the batch size was equal to 16. The mean square error (MSE) was chosen as the loss function, and the same reward function from Section 2.1 was chosen for success validation. As a noise scheduler, we used the DDPM scheduler with a glide cosine scheduler (i.e., `squaredcos_cap_v2`) and a step number of 50. After each subsequent 1000 iterations, the model was validated on 50 episodes with a positioned object according to the pose sampling algorithm from Section 3.2. The results of training the models can be seen in Fig. 9, which illustrates their convergence, as well as their high efficiency in capturing randomly located objects. The efficiency is close to 80%, which proves the applicability of the constructed pipeline for training a diffusion model to capture objects in complex unfamiliar scenarios. An illustration of examples of actions predicted by the diffusion model for each of three objects can be seen in Fig. 10.

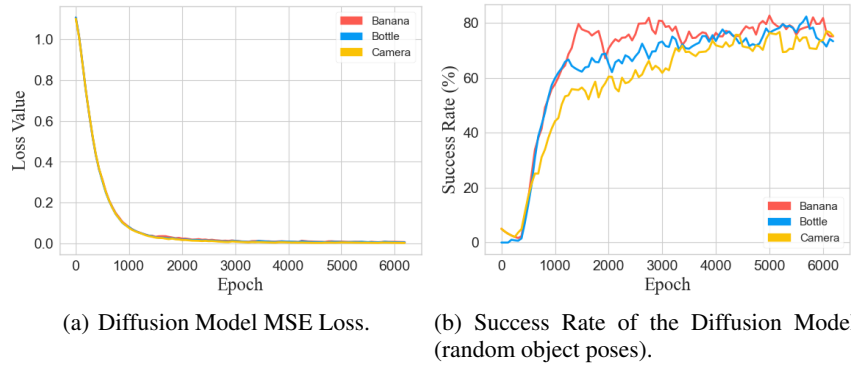


Figure 9: Diffusion Model Loss and Success Rate during training. Mean Success Rate is a mean percentage of transitions that have a success reward during validation.

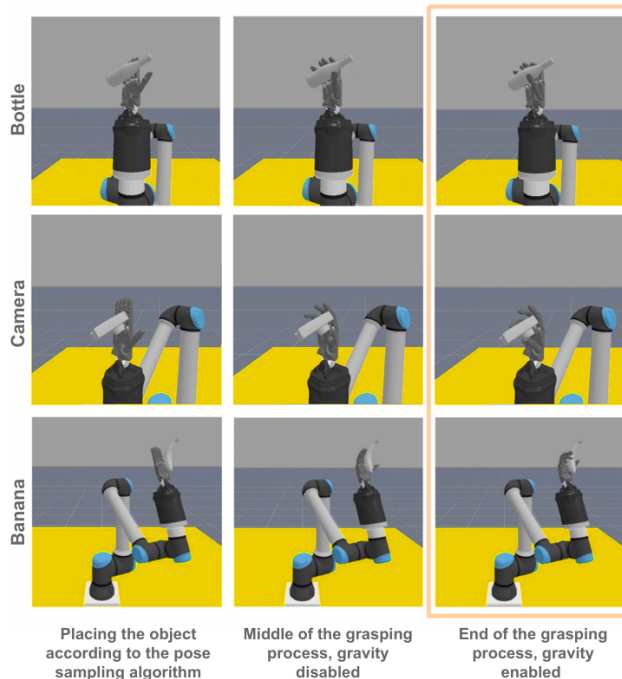


Figure 10: Example of grasping process with trained Diffusion Model.

4 Conclusion

In this paper, we demonstrate the effectiveness of training a compact diffusion model for dexterous robot grasping using a large-scale DexGraspNet dataset and refining it with Reinforcement Learning. Our pipeline integrates a lightweight RL agent to refine samples from the dataset, improving the quality and stability of grasping examples for diffusion policy learning. The trained model achieves a high success rate (about 80%) in grasping randomly placed objects, demonstrating its robustness and generalization ability.

Our approach significantly reduces the need for manual data collection to efficiently train lightweight diffusion models for dexterous multi-finger grasping manipulation. It can also be useful, for example, for training auxiliary for VLA diffusion models such as the one described in the aforementioned work [20], which demonstrates high performance when integrated. To train such diffusion models, it is now possible to avoid assembling small datasets for each specific scenario (about 30-40 examples), but instead to adapt ready-made datasets in a simulation environment using an RL agent. Given a

description of the environmental conditions and the agent’s task, the resulting adapted datasets will satisfy the requirements and be easily scalable. The pose sampling algorithm can be used to increase the number of samples of the datasets and to increase their diversity.

Future plans include adding more multimodal data for training, integrating the approach with Vision-Language-Action (VLA) models, and testing it in a real-world environment. Due to its flexibility, the pipeline can be easily integrated to train a variety of robotic tasks in different environments, increasing generalization and robustness for real-world applications.

References

- [1] J. Ho, A. Jain, and P. Abbeel. Denoising diffusion probabilistic models, 2020. URL <https://arxiv.org/abs/2006.11239>.
- [2] M. Czerkawski and C. Tachtatzis. Exploring the capability of text-to-image diffusion models with structural edge guidance for multispectral satellite image inpainting. *IEEE Geoscience and Remote Sensing Letters*, 21:1–5, 2024. ISSN 1558-0571. doi:10.1109/lgrs.2024.3370212. URL <http://dx.doi.org/10.1109/LGRS.2024.3370212>.
- [3] J. Ho, T. Salimans, A. Gritsenko, W. Chan, M. Norouzi, and D. J. Fleet. Video diffusion models, 2022. URL <https://arxiv.org/abs/2204.03458>.
- [4] Z. Kong, W. Ping, J. Huang, K. Zhao, and B. Catanzaro. Diffwave: A versatile diffusion model for audio synthesis, 2021. URL <https://arxiv.org/abs/2009.09761>.
- [5] X. Liu, K. Y. Ma, C. Gao, and M. Z. Shou. Diffusion models in robotics: A survey. 2025. URL <https://github.com/showlab/Awesome-Robotics-Diffusion.git>.
- [6] J. Hua, L. Zeng, G. Li, and Z. Ju. Learning for a robot: Deep reinforcement learning, imitation learning, transfer learning. *Sensors*, 21:1278, 02 2021. doi:10.3390/s21041278.
- [7] T. Eimer, M. Lindauer, and R. Raileanu. Hyperparameters in reinforcement learning and how to tune them, 2023. URL <https://arxiv.org/abs/2306.01324>.
- [8] S. Belkhale, Y. Cui, and D. Sadigh. Data quality in imitation learning, 2023. URL <https://arxiv.org/abs/2306.02437>.
- [9] C. Chi, Z. Xu, S. Feng, E. Cousineau, Y. Du, B. Burchfiel, R. Tedrake, and S. Song. Diffusion policy: Visuomotor policy learning via action diffusion, 2024. URL <https://arxiv.org/abs/2303.04137>.
- [10] W. Xiao, T.-H. Wang, C. Gan, and D. Rus. Safediffuser: Safe planning with diffusion probabilistic models, 2023. URL <https://arxiv.org/abs/2306.00148>.
- [11] T. Power, R. Soltani-Zarrin, S. Iba, and D. Berenson. Sampling constrained trajectories using composable diffusion models. In *IROS 2023 Workshop on Differentiable Probabilistic Robotics: Emerging Perspectives on Robot Learning*, 2023. URL <https://openreview.net/forum?id=UAylEpIMNE>.
- [12] R. Tian, Y. Wu, C. Xu, M. Tomizuka, J. Malik, and A. Bajcsy. Maximizing alignment with minimal feedback: Efficiently learning rewards for visuomotor robot policy alignment, 2024. URL <https://arxiv.org/abs/2412.04835>.
- [13] J. Yang, C. Glossop, A. Bhorkar, D. Shah, Q. Vuong, C. Finn, D. Sadigh, and S. Levine. Pushing the limits of cross-embodiment learning for manipulation and navigation, 2024. URL <https://arxiv.org/abs/2402.19432>.
- [14] H. Ha, Y. Gao, Z. Fu, J. Tan, and S. Song. Umi on legs: Making manipulation policies mobile with manipulation-centric whole-body controllers, 2024. URL <https://arxiv.org/abs/2407.10353>.

- [15] A. Sridhar, D. Shah, C. Glossop, and S. Levine. Nomad: Goal masked diffusion policies for navigation and exploration, 2023. URL <https://arxiv.org/abs/2310.07896>.
- [16] J. Liu, M. Stamatopoulou, and D. Kanoulas. Dipper: Diffusion-based 2d path planner applied on legged robots, 2024. URL <https://arxiv.org/abs/2310.07842>.
- [17] T. Wu, M. Wu, J. Zhang, Y. Gan, and H. Dong. Graspgf: Learning score-based grasping primitive for human-assisting dexterous grasping, 2025. URL <https://arxiv.org/abs/2309.06038>.
- [18] Z. Zhang, L. Zhou, C. Liu, Z. Liu, C. Yuan, S. Guo, R. Zhao, M. H. A. Jr., and F. E. Tay. Dexgrasp-diffusion: Diffusion-based unified functional grasp synthesis method for multi-dexterous robotic hands, 2024. URL <https://arxiv.org/abs/2407.09899>.
- [19] Z. Chen, S. Chen, E. Arlaud, I. Laptev, and C. Schmid. Vividex: Learning vision-based dexterous manipulation from human videos, 2025. URL <https://arxiv.org/abs/2404.15709>.
- [20] C. Pan, K. Junge, and J. Hughes. Vision-language-action model and diffusion policy switching enables dexterous control of an anthropomorphic hand, 2024. URL <https://arxiv.org/abs/2410.14022>.
- [21] K. Junge and J. Hughes. Robust anthropomorphic robotic manipulation through biomimetic distributed compliance, 2024. URL <https://arxiv.org/abs/2404.05262>.
- [22] R. Wang, J. Zhang, J. Chen, Y. Xu, P. Li, T. Liu, and H. Wang. Dexgraspnet: A large-scale robotic dexterous grasp dataset for general objects based on simulation, 2023. URL <https://arxiv.org/abs/2210.02697>.
- [23] Shadow Robot Company. Shadow robot company: Advanced robotic hands, 2024. URL <https://www.shadowrobot.com>. <https://www.shadowrobot.com> [Accessed: 20-April-2025].
- [24] T. P. Lillicrap, J. J. Hunt, A. Pritzel, N. Heess, T. Erez, Y. Tassa, D. Silver, and D. Wierstra. Continuous control with deep reinforcement learning, 2019. URL <https://arxiv.org/abs/1509.02971>.
- [25] J. Ho, A. Jain, and P. Abbeel. Denoising diffusion probabilistic models, 2020. URL <https://arxiv.org/abs/2006.11239>.
- [26] O. Ronneberger, P. Fischer, and T. Brox. U-net: Convolutional networks for biomedical image segmentation, 2015. URL <https://arxiv.org/abs/1505.04597>.
- [27] S. Tao, F. Xiang, A. Shukla, Y. Qin, X. Hinrichsen, X. Yuan, C. Bao, X. Lin, Y. Liu, T. kai Chan, Y. Gao, X. Li, T. Mu, N. Xiao, A. Gurha, Z. Huang, R. Calandra, R. Chen, S. Luo, and H. Su. Maniskill3: Gpu parallelized robotics simulation and rendering for generalizable embodied ai, 2024. URL <https://arxiv.org/abs/2410.00425>.